THE IMPEDANCE CHARACTERISTICS OF A COAXIAL TEM-LINE ANTENNA

Jerry Neal Layl

NAVAL POSTGRADUATE SCHOOL
Monterey, California

THESIS

THE IMPEDANCE CHARACTERISTICS
OF
A COAXIAL TEM-LINE ANTENNA

by

Jerry Neal Layl

Thesis Advisor: R.W. Adler

June 1972

T

The Impedance Characteristics

of

A Coaxial TEM-line Antenna

by

Jerry Neal Layl
Lieutenant, United States Navy
B.S.E.E., Purdue University, 1968

Submitted in partial fulfillment of the
requirements for the degree of

MASTER OF SCIENCE IN ELECTRICAL ENGINEERING

from the

NAVAL POSTGRADUATE SCHOOL
June 1972

ABSTRACT

The coaxial TEM-line antenna is a low-profile, light-weight, simply constructed antenna that can be easily mounted on a wide variety of conducting surfaces. It is a low to medium gain antenna element capable of operation in broadside or frequency scanning modes.

This paper presents a method of determining the impedance characteristics of a single flush mounted radiating gap.

Several radiation patterns are presented to illustrate beam shape and scanning. The Brillouin or ω-β diagram is used to relate the frequency scanning properties to periodic structure theory.

TABLE OF CONTENTS

LIST OF FIGURES

I. INTRODUCTION

A. DESCRIPTION OF ANTENNA

The TEM-line antenna is a low-profile, frequency scanning antenna that derives its name from the transverse electric and magnetic (TEM) transmission line from which it is constructed [1]. In its simplest form the TEM-line antenna consists of a coaxial transmission line with periodic interruptions in its outer conductor, which is bonded to a large metal ground plane and fitted with feed and termination connections as illustrated in Figure 1. Energy is fed into one end of the structure, radiates from the gaps as it travels down the line and at the end of the line is reflected, absorbed or retransmitted depending on the termination. The number of traveling waves on the structure determines the number of beams or lobes in the far field pattern [2,3]. The frequency scanning feature of the TEM-line antenna with a short circuit termination is shown in Figure 2.

B. REVIEW OF RELATED WORK

Several studies of TEM-line antennas have been done at the Electro Science Laboratory of the Ohio State University [2,3,4,5,6,7,8]. The bulk of the Ohio State work was with TEM-line antenna configurations with small rectangular radiating elements as shown in Figure 3. The behavior of the numerous variations in gap geometry does, however,

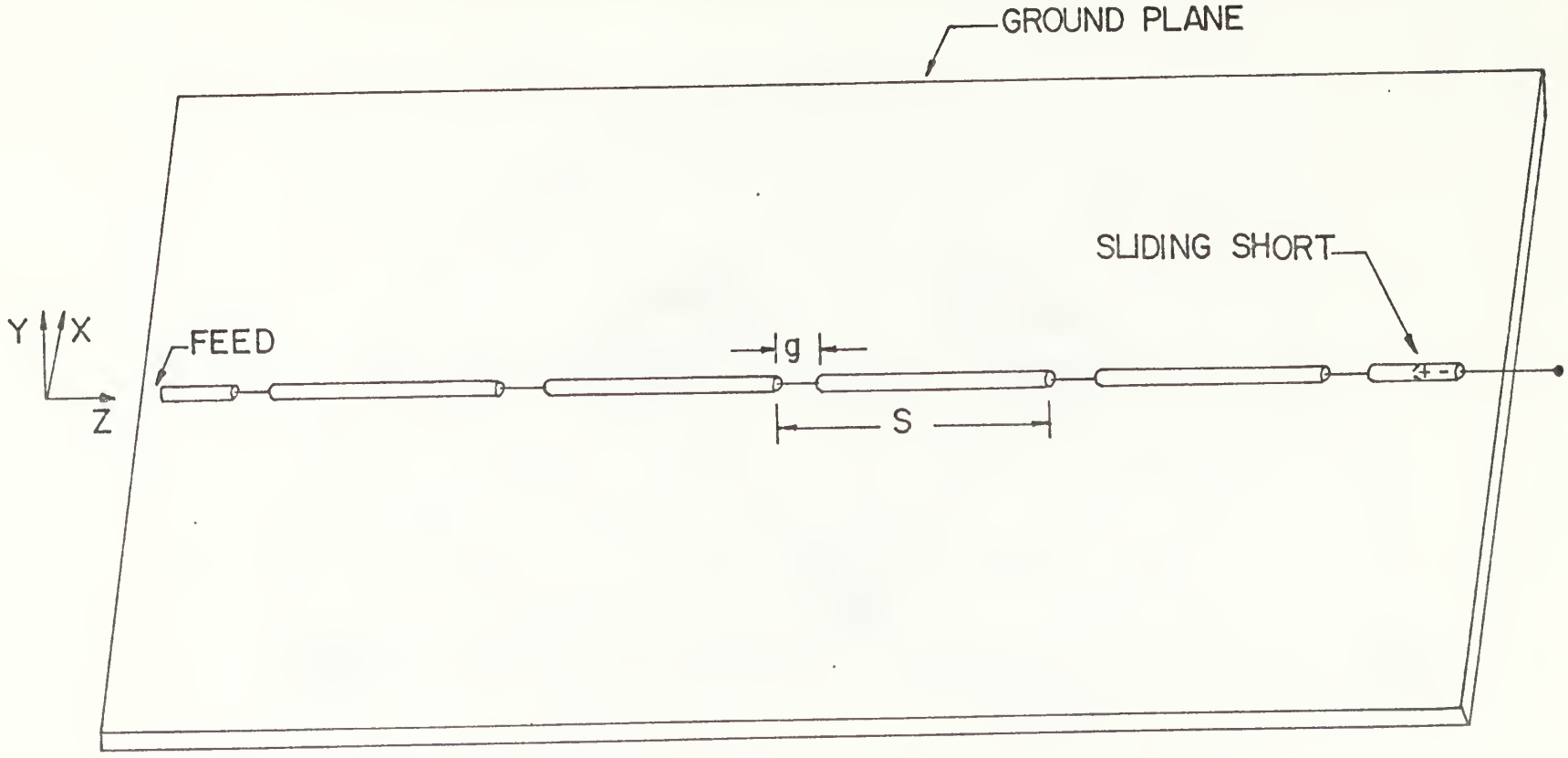

FIGURE 1. SURFACE MOUNTED COAXIAL TEM-LINE ANTENNA

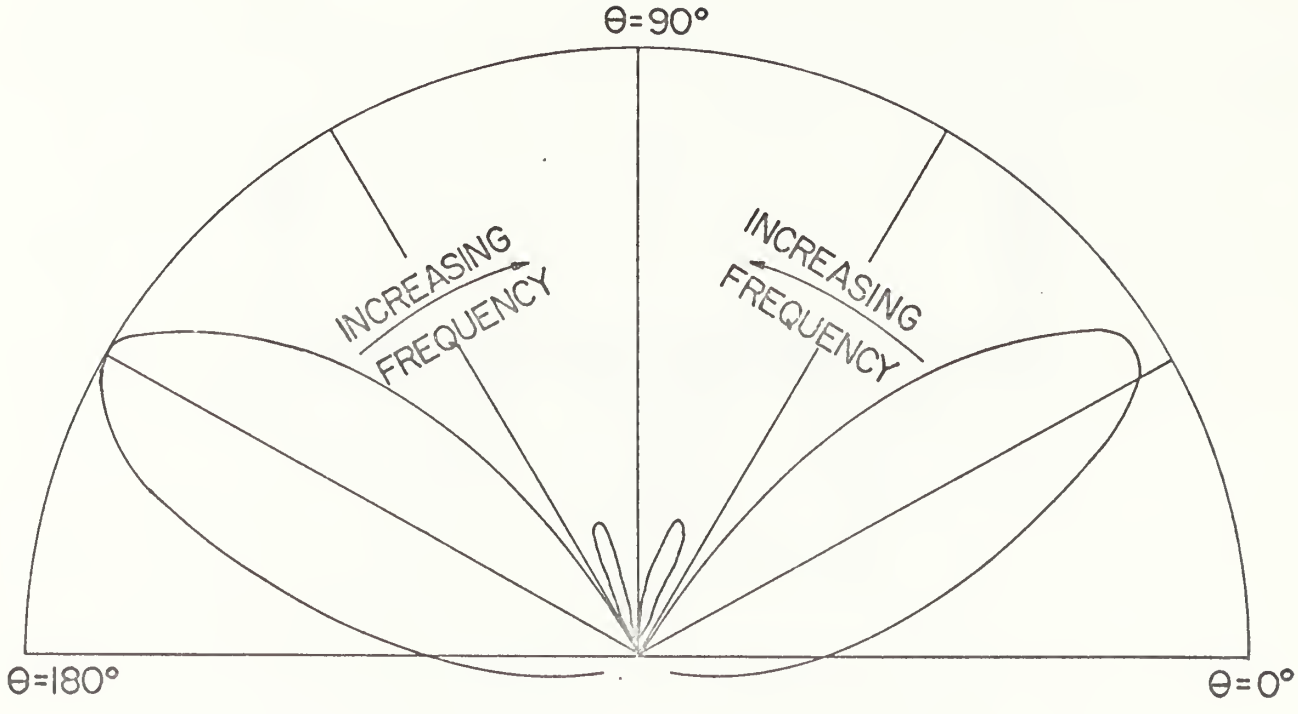

FIGURE 2. FAR FIELD RADIATION PATTERN FOR THE SURFACE MOUNTED TEM-LINE ANTENNA; SHORT CIRCUIT TERMINATION.

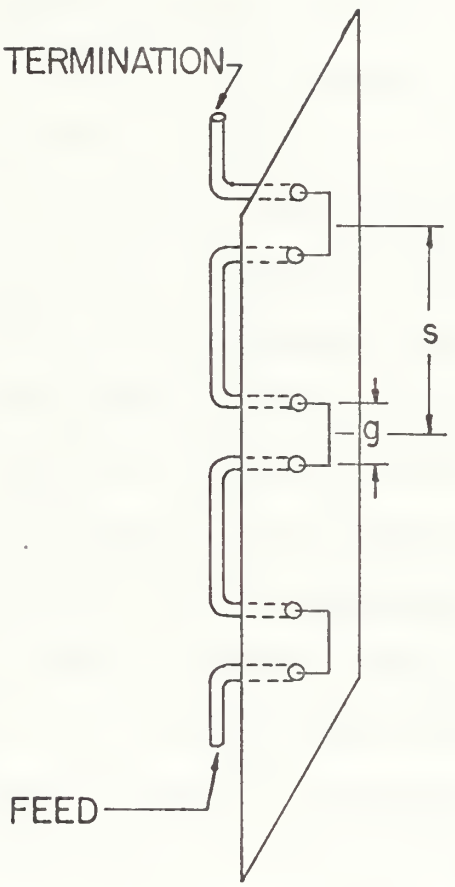

FIGURE 3. TEM-LINE ANTENNA WITH RECTANGULAR RADIATING ELEMENTS

indicate a common radiation mechanism for all the members. J. R. Copeland obtained good correlation between theoretical and measured results based on a small rectangular half-loop as the radiating element [1]. Copeland further suggested that various geometries of radiating elements may be approximated by a small rectangular half-loop of equivalent area if the total conductor length of the half-loop is less than $\lambda/4$ and constant current is assumed. In a study done at the Naval Postgraduate School, L. W. Patak has shown, although not conclusively, that Copeland's hypothesis is not applicable when the radiating element is completely flush mounted [9]. J. R. Copeland also studied the flush mounted TEM-line antenna mounted on the flat surface of a ground plane (Figure 1) and also on the edge of a ground plane as shown in Figure 4. The edge mounted version demonstrated the same type of scanning from grazing through broadside in the same frequency interval as the surface mounted version. The results were surprising in that there was little change in antenna performance when the slotted coaxial cable was moved to the edge of the ground plane. The chief difference was broader H-plane coverage of the edge mounted version and its imperfect suppression of the forward lobe in the low frequency region.

C. STATEMENT OF PROBLEM

The edge mounted, low-profile TEM-line antenna is one of the simplest and most rugged versions. The object of this study is to investigate the impedance properties of a

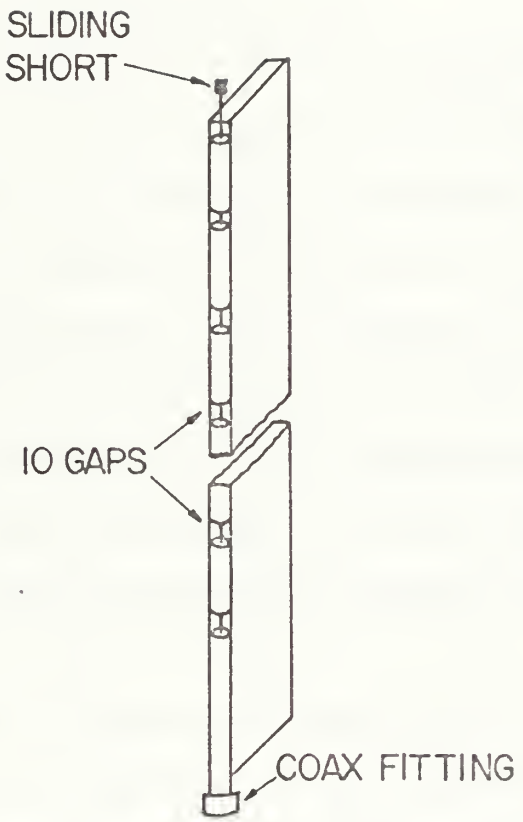

FIGURE 4. EDGE MOUNTED COAXIAL TEM-LINE ANTENNA

single flush mounted radiating gap. This paper, therefore, presents a method of determining the impedance characteristics of a single flush mounted gap as shown in Figure 5. The results of this study should further confirm or deny the equivalent rectangular half-loop hypothesis.

D. SCOPE AND LIMITATIONS OF WORK

This study was limited to the determination of the impedance characteristics of a single 0.0625λ (2.5 cm) gap. A five gap TEM-line antenna was constructed for use in determining the radiation resistance of the single gap [10]. The five gap structure, shown in Figure 6, was designed for broadside operation at 750 MHz with 0.0625λ (2.5 cm) gaps placed 0.7λ (28 cm) apart. The impedance characteristics of the single gaps were then determined using time domain reflectometry (TDR) methods and periodic structure theory [11,12].

As a further attempt to understand the operation of the flush mounted TEM-line antenna, power measurements were made on both structures, an ω-β diagram was calculated and plotted, and radiation patterns for the five gap structure were recorded.

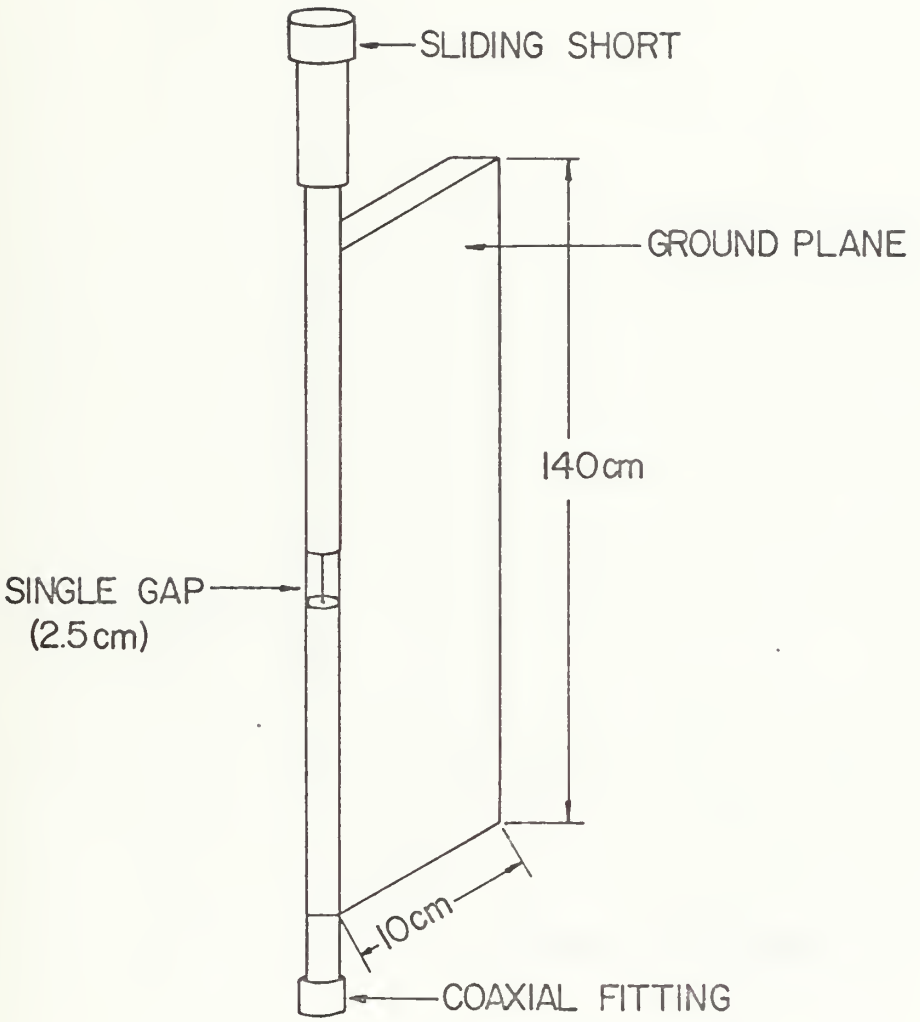

FIGURE 5. SINGLE GAP EDGE MOUNTED COAXIAL TEM-LINE ANTENNA

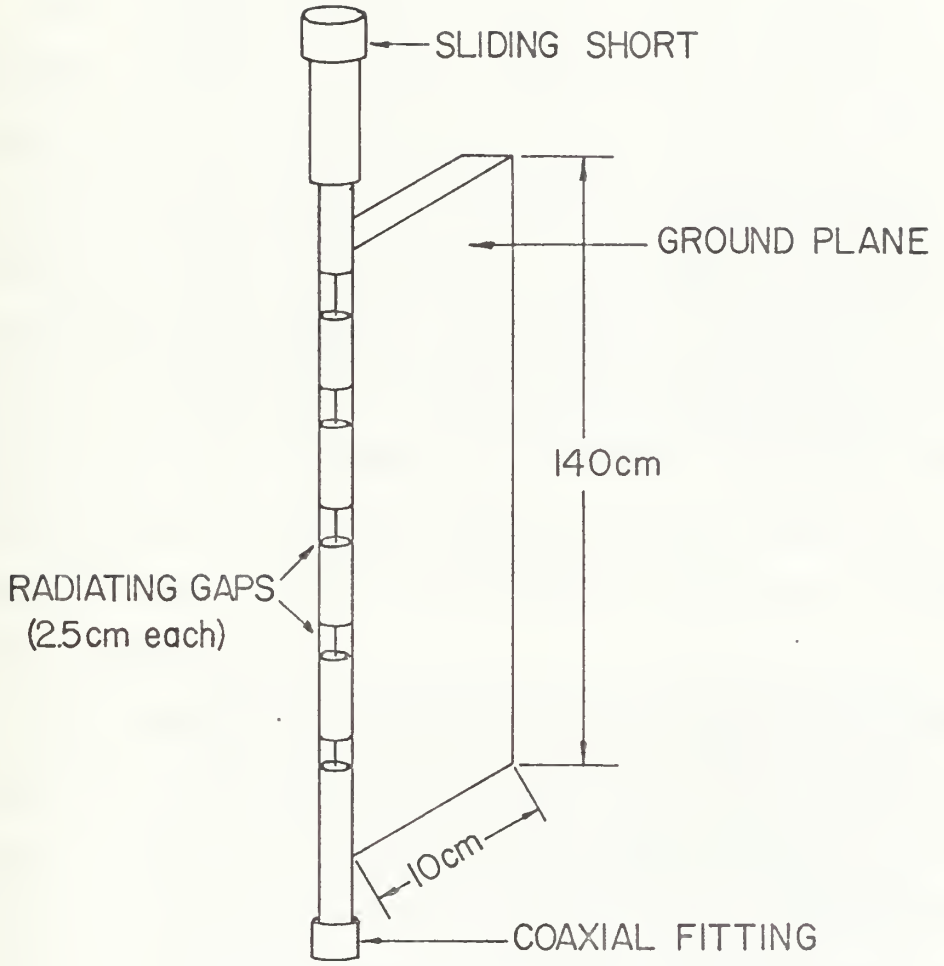

FIGURE 6. FIVE GAP EDGE MOUNTED COAXIAL TEM-LINE ANTENNA

II. ANALYSIS

A. DETERMINATION OF GAP CHARACTERISTICS

The TDR measurements indicated that the single radiating gap was inductive. It was assumed the single gap could be represented by a series inductor and resistor. The value of the series inductor was easily measured using TDR techniques as 5.2×10^{-9} henry[11]. The series resistance which represents the radiation resistance of the gap was calculated by considering the five gap antenna as a lightly loaded periodic transmission line and using TDR techniques. Photographs of the TDR presentations for the single gap radiator and the five gap radiator are shown in Figures 7 and 8 respectively.

The equations required for the calculation of the radiation resistance were derived by calculating the propagation constant for cascaded two-port networks in terms of the open circuit parameters [Z] and then applying the results to a transmission line with a series impedance $[Z_s]$.

Consider an infinite number of two-ports or unit cells in cascade:

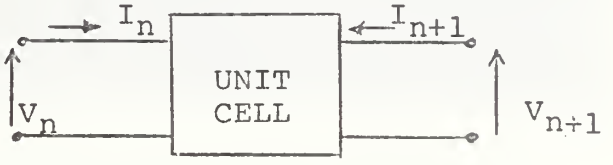

$$(1) \quad V_n = Z_{11}I_n + Z_{12}I_{n+1}$$

$$(2) \quad V_{n+1} = Z_{21}I_n + Z_{22}I_{n+1} \quad .$$

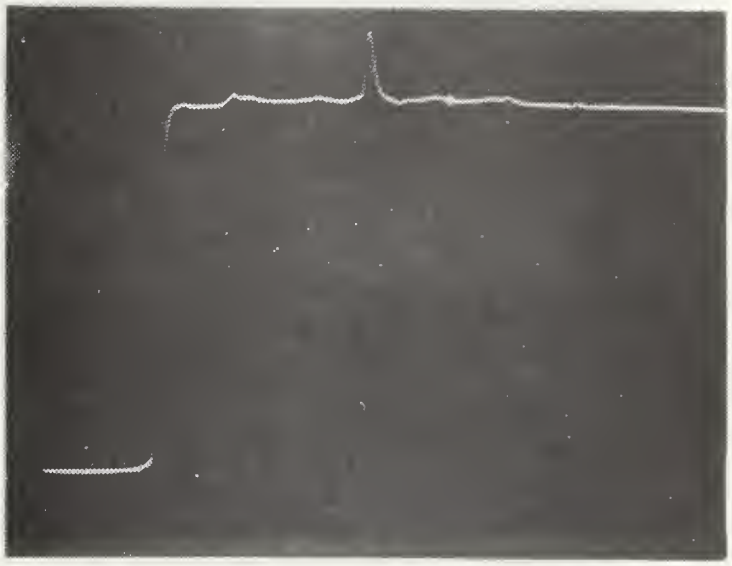

A. 4 nsec/cm horizontal deflection
.5 v/cm vertical deflection

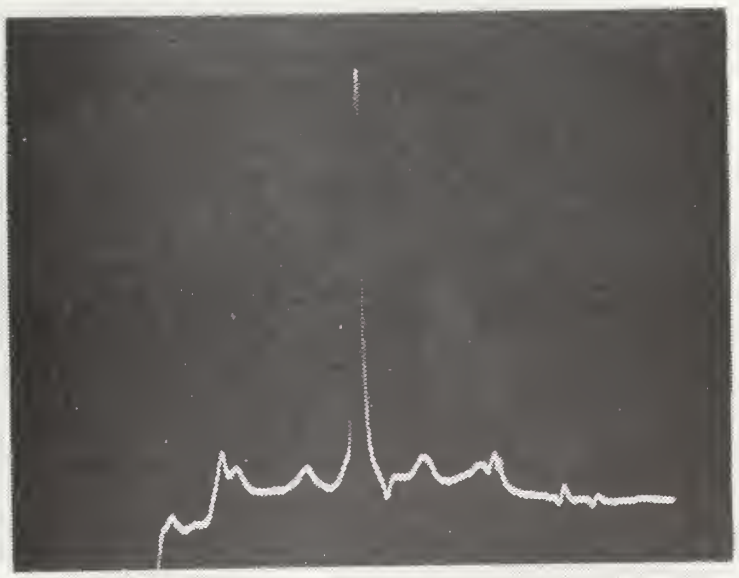

B. 4 nsec/cm horizontal deflection
.05 v/cm vertical deflection

FIGURE 7. TDR PRESENTATION OF THE SINGLE GAP ANTENNA

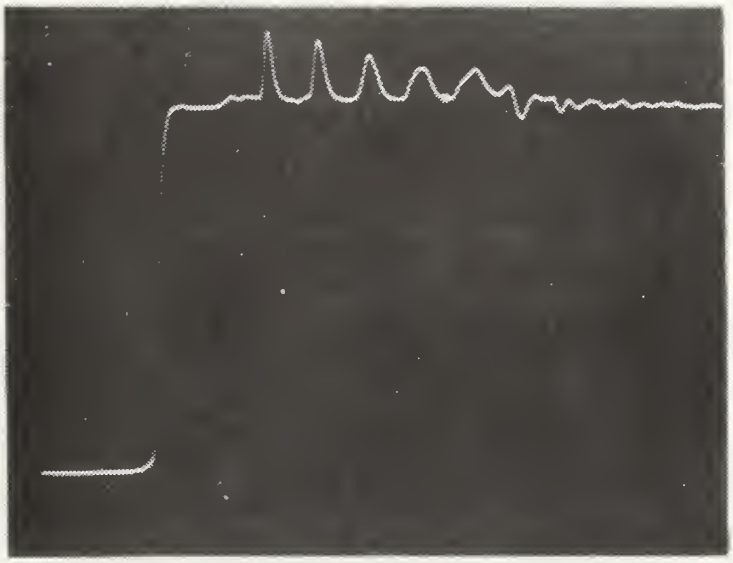

A. 4 nsec/cm horizontal deflection
.5 v/cm vertical deflection

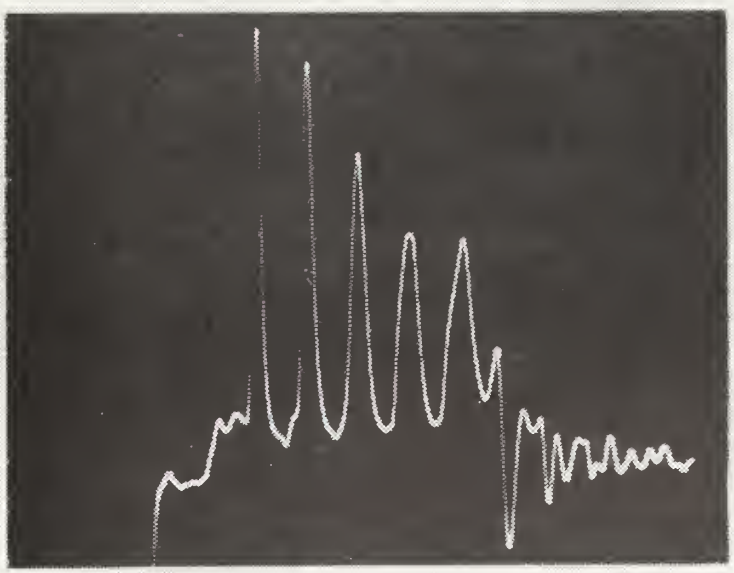

B. 4 nsec/cm horizontal deflection
.05 v/cm vertical deflection

FIGURE 8. TDR PRESENTATION OF THE FIVE GAP ANTENNA

By Floquet's Theorem, the currents and voltages differ only by a phase shift, therefore:

(3) $I_{n+1} = -I_n \varepsilon^{-\gamma_o L}$ $\quad \gamma_o$ = propagation constant

(4) $V_{n+1} = V_n \varepsilon^{-\gamma_o L}$ $\quad L$ = length of unit cell.

By substituting (3) and (4) into (1) and (2), then equating (1) and (2):

(5) $\text{COSH } \gamma_o L = \dfrac{Z_{11} + Z_{22}}{2Z_{12}} = \dfrac{Z_{11} + Z_{22}}{2Z_{21}}$.

Applying the above result to a transmission line with series impedance $[Z_s]$:

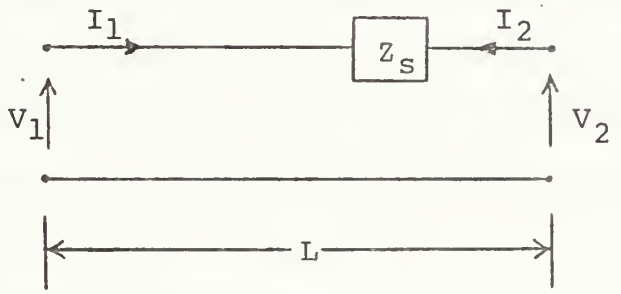

(6) $Z_{11} = \left.\dfrac{V_1}{I_1}\right|_{I_2=0} = Z_o \text{ COTH } \gamma L$ $\quad \gamma$ = propagation constant of the loaded line

(7) $Z_{22} = \left.\dfrac{V_2}{I_2}\right|_{I_1=0} = Z_o \text{ COTH } \gamma L + Z_s$

(8) $Z_{12} = \left.\dfrac{V_1}{I_2}\right|_{I_1=0} = Z_{21} = \left.\dfrac{V_2}{I_1}\right|_{I_2=0} = \dfrac{Z_o}{\text{SINH } \gamma L}$

By substituting (6), (7), and (8) into (5):

$$(9)\quad \text{COSH } \gamma_o L = \text{COSH } \gamma L + \frac{Z_s}{2Z_o} \text{ SINH } \gamma L \quad .$$

For a lossless line, $\gamma = j\beta$, equation (9) becomes:

$$(10)\quad \text{COSH } \gamma_o L = \text{COS } \beta L + j \frac{z_s}{2} \text{ SIN } \beta L$$

$$z_s = \frac{Z_s}{Z_o} = r_s + jx_s \quad .$$

Expanding and equating real and imaginary parts:

$$(11)\quad \text{COSH } \alpha_o L \text{ COS } \beta_o L = \text{COS } \beta L - \frac{x_s}{2} \text{ SIN } \beta L$$

$$(12)\quad \text{SINH } \alpha_o L \text{ SIN } \beta_o L = \frac{r_s}{2} \text{ SIN } \beta L \quad .$$

Equations (11) and (12) relate the cascaded two-port networks and the transmission line with series impedance $[Z_s]$ if the loss in the coaxial cable is assumed to be very small. Two special cases need to be considered to make further simplifying assumptions.

Case 1: Pure reactive loading, $r_s=0$.

If $r_s=0$, then $\alpha_o L=0$, COSH $\alpha_o L=1$, and equation (11) becomes:

$$(13)\quad \text{COS } \beta_o L = \text{COS } \beta L - \frac{x_s}{2} \text{ SIN } \beta L \quad .$$

In an ω-β diagram for a lightly loaded line for the low frequency asymptote the following assumptions may be made [12]:

$\beta_o L << 1$; $\beta L << 1$; $\cos \beta_o L \simeq 1 - \frac{(\beta_o L)^2}{2}$;

$\cos \beta L \simeq 1 - \frac{(\beta L)^2}{2}$; $\sin \beta L \simeq \beta L$.

Equation (13) becomes:

$$(14) \quad 1 - \frac{(\beta_o L)^2}{2} = 1 - \frac{(\beta L)^2}{2} - \frac{x_s}{2} \beta L \quad .$$

Letting $x_s = \frac{\omega L_s}{Z_o}$, $\beta = \omega L_\ell C_\ell$, and $Z_o = \frac{L_\ell}{C_\ell}$, where C_ℓ and L_ℓ are the capacitance per unit length and the inductance per unit length of the coaxial cable, solving equation (14) for β_o gives:

$$(15) \quad \beta_o = C_\ell \left(L_\ell + \frac{L_s}{L} \right) \quad \text{for } r_s = 0 \quad .$$

Case 2: $0 < r_s << 1$, $L_s << L_\ell$.

For $\beta_o L << 1$, $\beta L << 1$, and $\alpha_o L << 1$ as in Case 1, equation (12) becomes:

$$(\alpha_o L)(\beta_o L) \simeq \frac{r_s}{2} (\beta L)$$

$$\alpha_o L \simeq \frac{r_s}{2} \frac{L_\ell}{L_\ell + \frac{L_s}{2}}$$

$$(16) \quad \alpha_o L \simeq \frac{r_s}{2} \left(1 - \tfrac{1}{2} \frac{L_s/L}{L_\ell} \right) \quad \text{for } r_s << 1, \; L_s << L_\ell \quad .$$

A check of the manufacturer's specifications for the coaxial cable used justifies the assumption that $L_s << L_\ell$ [13]. α_o was calculated from the TDR display of the five gap radiator as 0.82 db/m which justifies the assumption that $\alpha_o L << 1$. The series resistance, R_s was calculated from (16) as:

$$r_s = .0538$$

$$R_s = Z_o r_s = 2.69\Omega \quad .$$

The circuit representation of the gap is shown in Figure 9.

B. ω-β DIAGRAM FOR THE TEM-LINE ANTENNA

The traveling wave behavior of a periodic structure is characterized by various regions of a Brillouin or ω-β diagram [14]. The ω-β diagram for the TEM-line antenna, shown in Figure 10, was prepared by programming Equation (13) on a Wang 500 Advanced Programming Calculator. The ω-β diagram is particularly useful in that it permits one to obtain a considerable amount of information without actually solving any field problems.

The ω-β diagram is a plot of radian frequency, ω, versus propagation constant, β, and for free space propagation, $\beta = \omega\sqrt{\mu\varepsilon} = k$. The phase velocity of a traveling wave in the semi-rigid coaxial cable is 0.7 times the speed of light which falls below the ω=k line on the diagram. The addition of the gaps to the coax is the same as adding periodic light loading elements. The light loading causes

the propagation constant, β , to become a complex quantity in certain regions called stopbands. Imaginary or complex β denotes attenuation which is observed in Figure 10 as the regions where the slopes of the curves go to zero. The propagation constant in a radiating structure is always complex, however, in the case of the five gap TEM-line antenna the loading is very light and the behavior is very nearly that of an enclosed lightly loaded line that does not radiate.

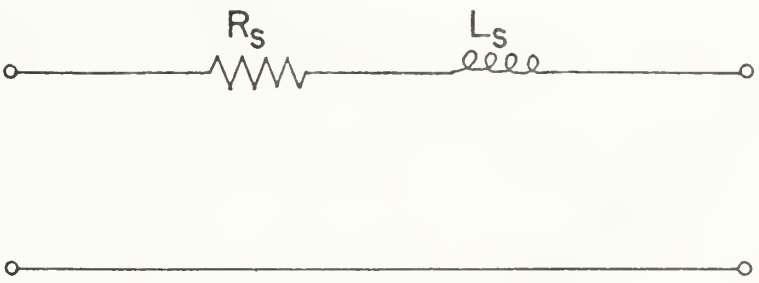

FIGURE 9. CIRCUIT ELEMENT REPRESENTATION OF A SINGLE GAP

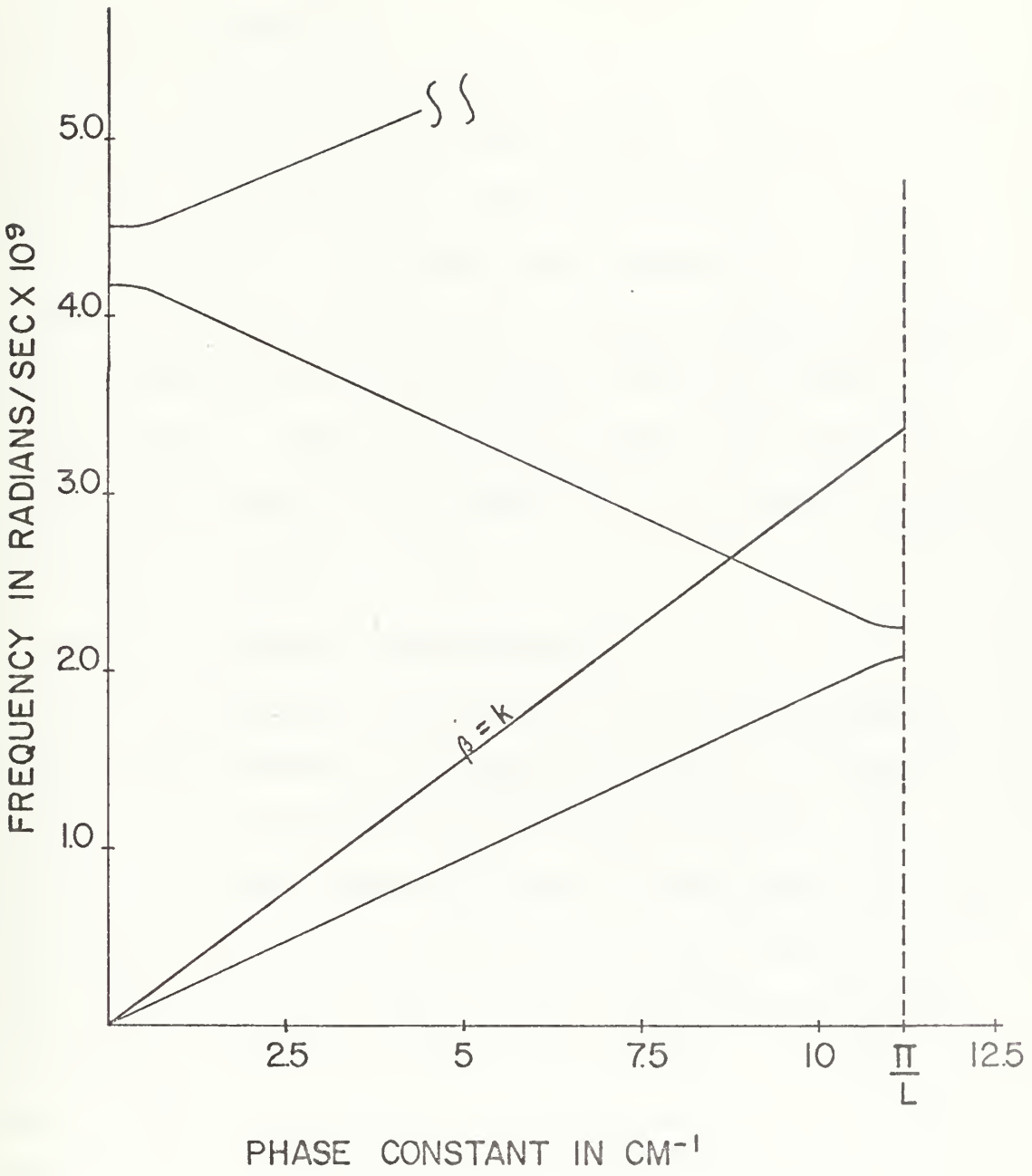

FIGURE 10. ω-β DIAGRAM OF THE COAXIAL TEM-LINE ANTENNA

III. MEASUREMENTS

A. POWER MEASUREMENTS

Power Measurements were made on the single gap and the five gap radiators in which the incident, reflected, and load powers were measured. The experimental set-up is shown in Figure 11. The data was normalized to a 50.0 milliwatt incident power and the radiated power was determined by subtracting reflected and load power from the incident power. The power data for both the single gap and five gap radiators was converted to dbm and is plotted in Figures 12 and 13.

B. PATTERN COMPARISON MEASUREMENTS

Far field E-plane patterns for the five gap antenna together with resonant $\lambda/2$ dipole patterns at the same frequency were recorded from 400 MHz to 850 MHz. The 400 MHz to 850 MHz frequency range includes the first two stop bands. The patterns for the five gap antenna were taken with a variable short circuit termination adjusted for maximum signal strength at the receiver. The only exception was the addition of a double stub tuner in the transmission line to the receiver for a single measurement at the design frequency, 750 MHz. The $\lambda/2$ dipole patterns were taken by replacing the five gap antenna with the dipole while maintaining all other conditions the same. A series attenuator was used so that both patterns could be presented

on the same plot. The most favorable comparison in which the five gap antenna pattern was approximately 2 db above the resonant $\lambda/2$ dipole pattern was obtained at the design frequency with both ends of the five gap antenna tuned.

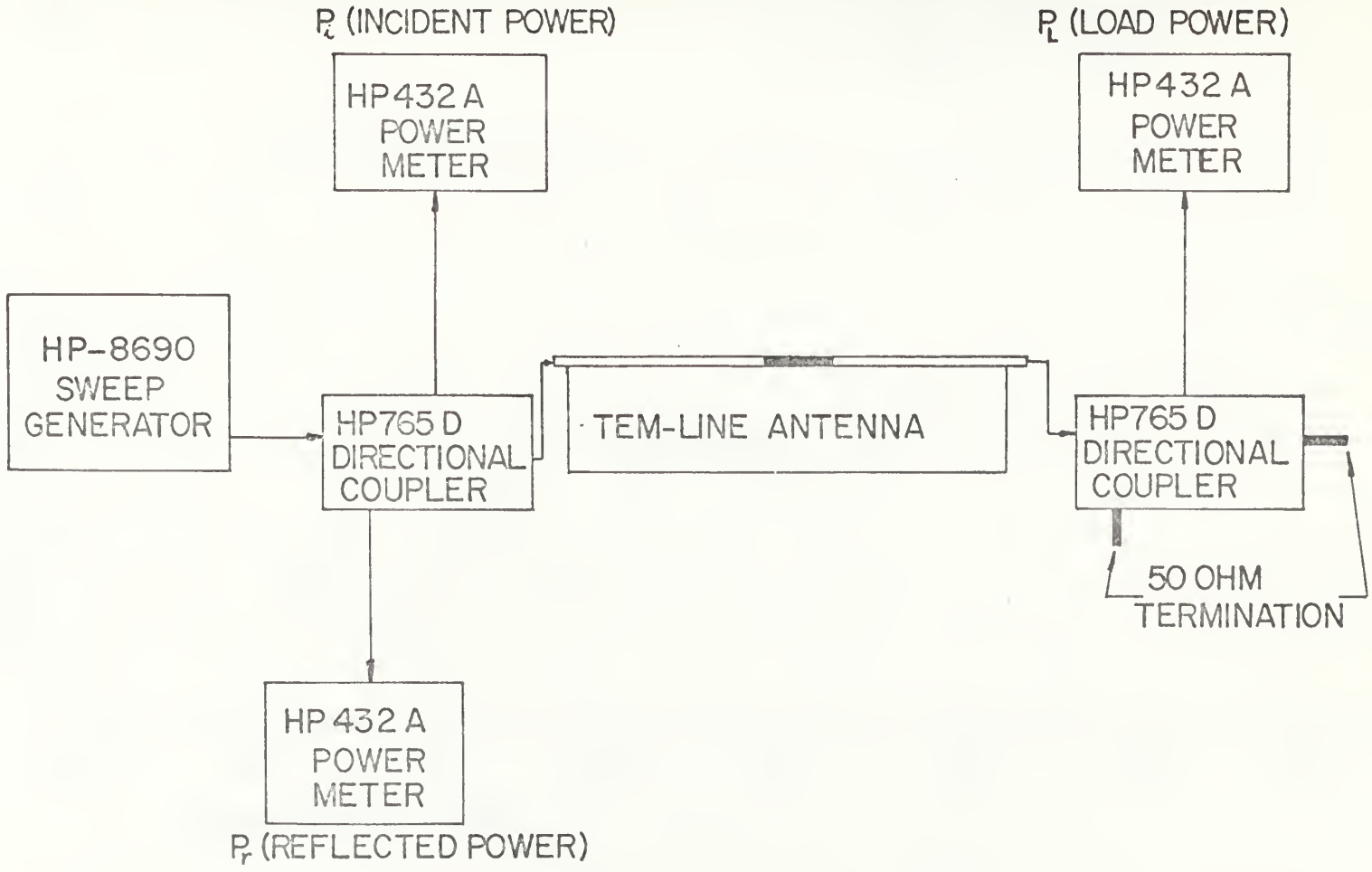

FIGURE 11. EXPERIMENTAL POWER MEASUREMENT SET-UP

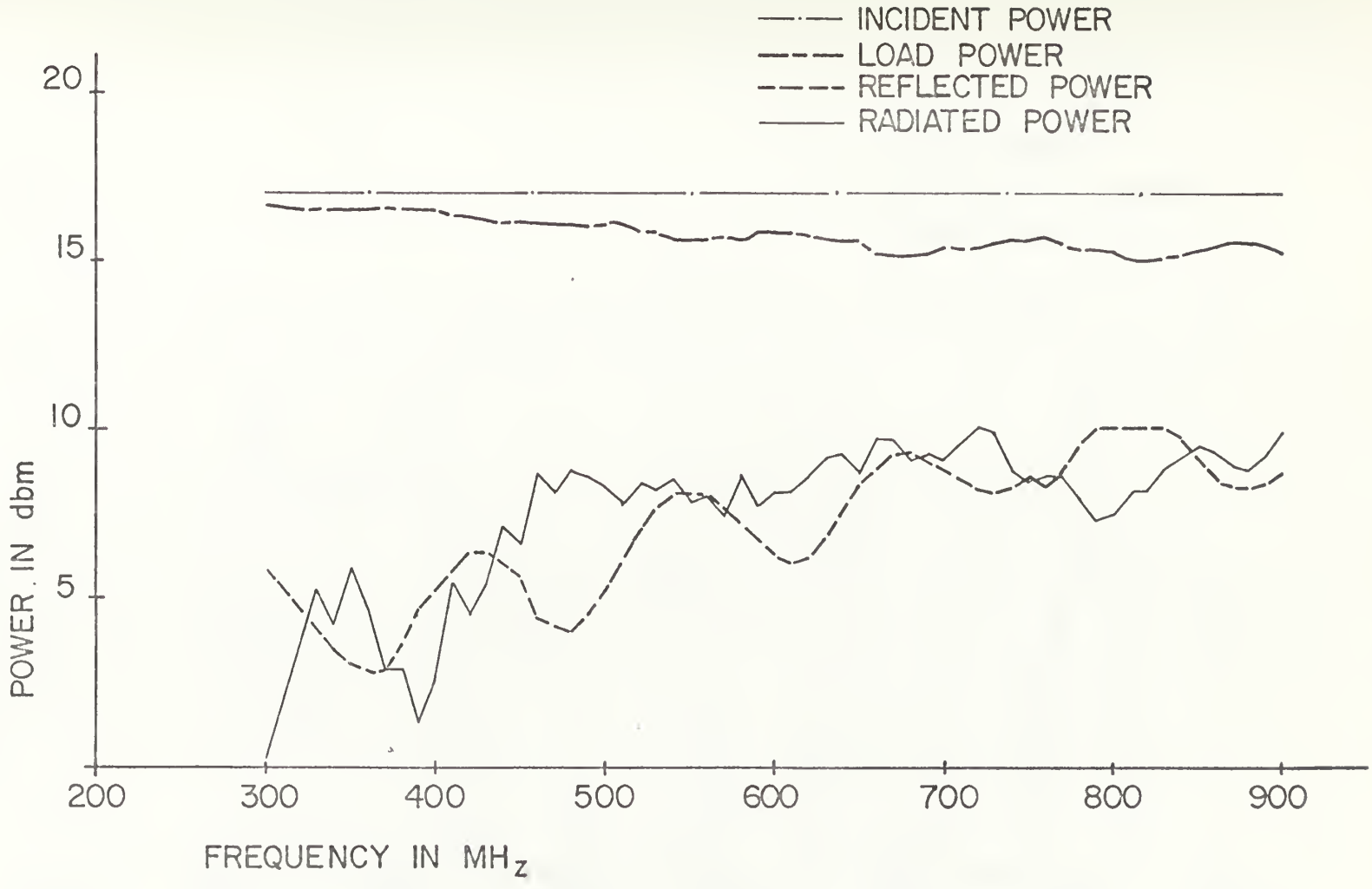

FIGURE 12. POWER IN THE SINGLE GAP RADIATOR

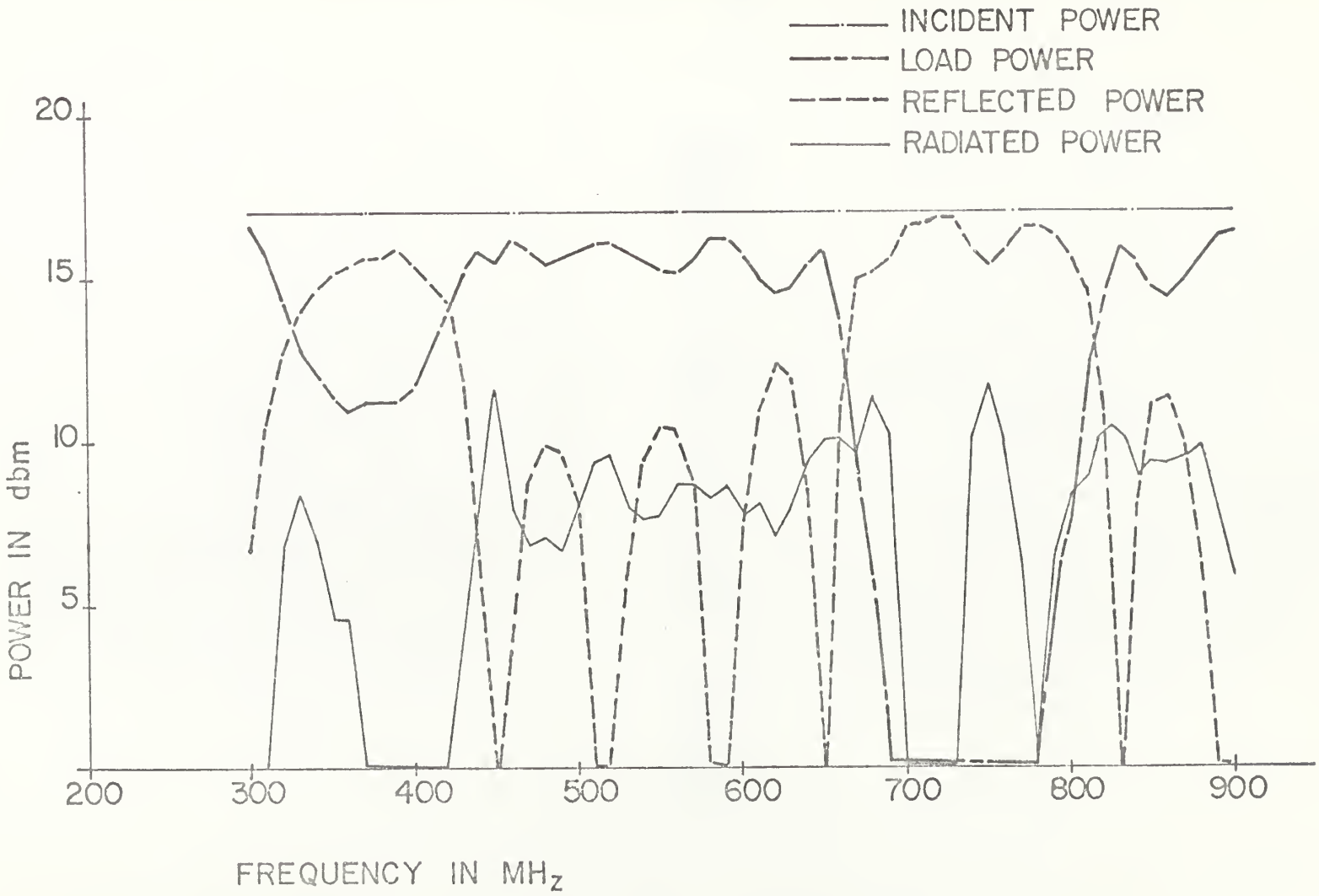

FIGURE 13. POWER IN THE FIVE GAP RADIATOR

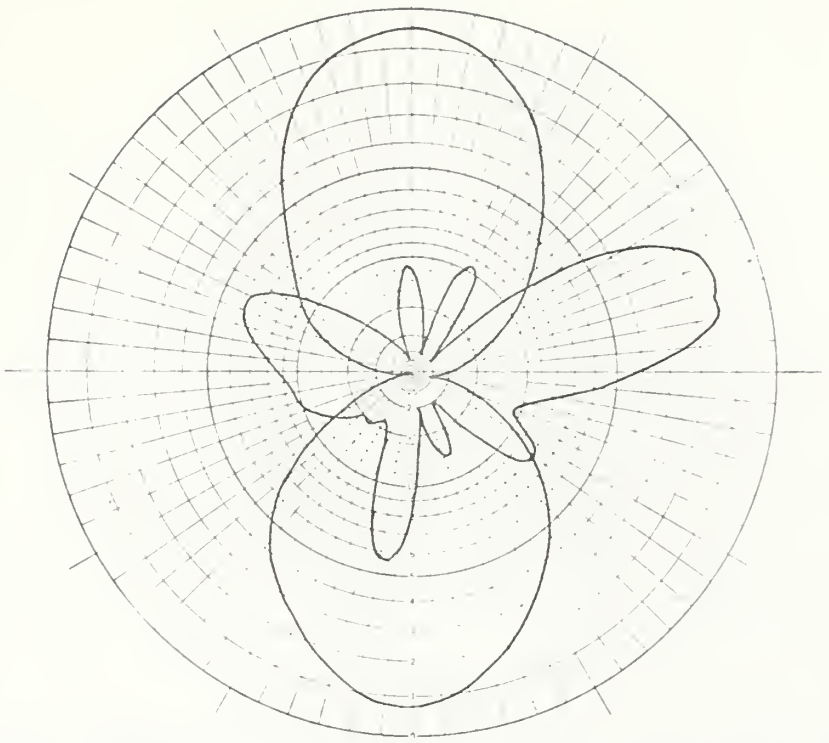

FIGURE 14. Radiation patterns of five gap antenna and resonant λ/2 dipole at 400 MHz. (TEM-line pattern 22 db down from λ/2.)

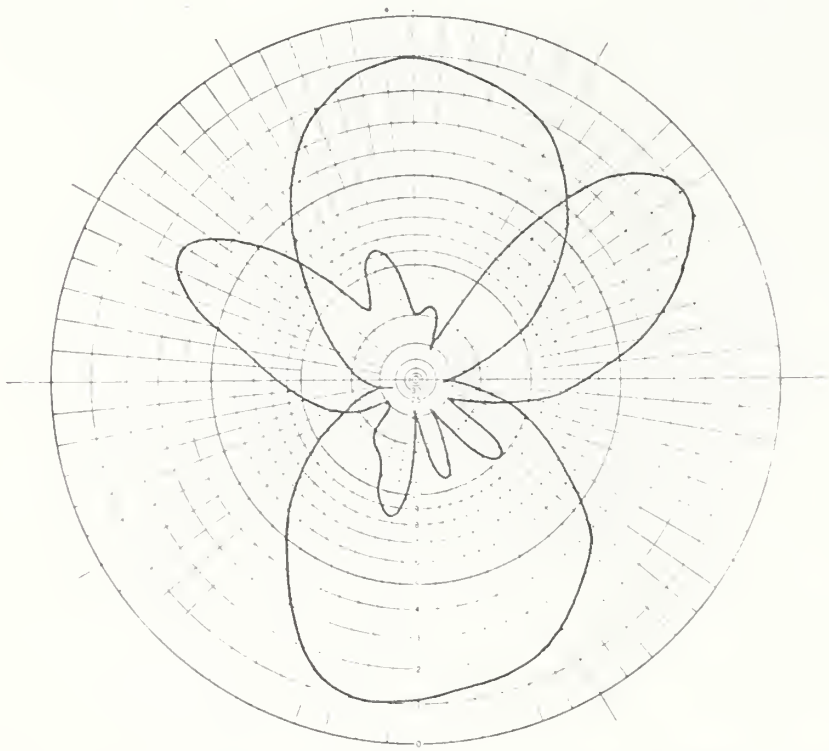

FIGURE 15. Radiation patterns of five gap antenna and resonant λ/2 dipole at 450 MHz. (TEM-line pattern 5 db down from λ/2.)

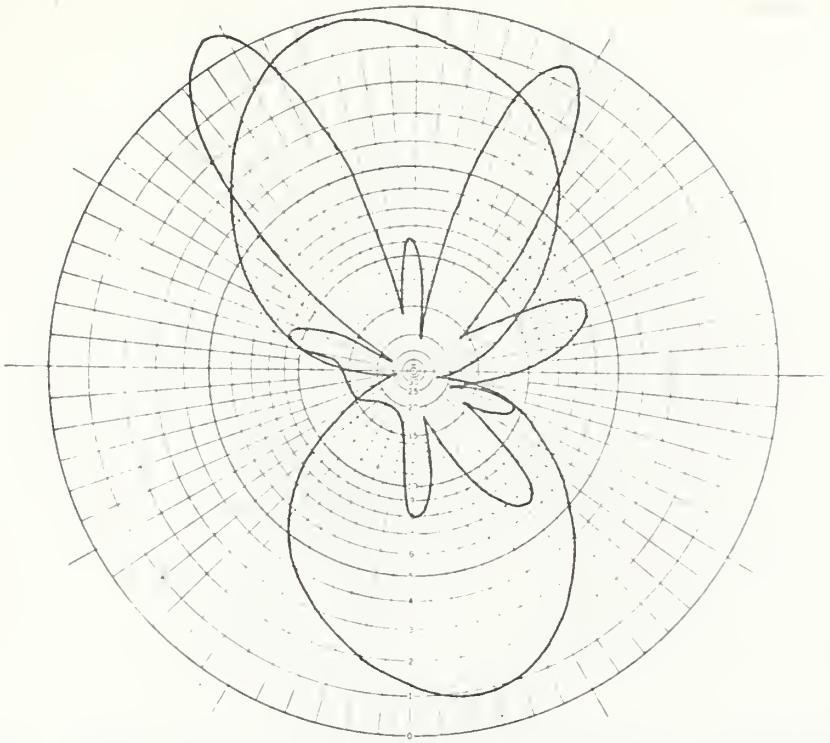

FIGURE 16. Radiation patterns of five gap antenna and resonant $\lambda/2$ dipole at 550 MHz. (TEM-line pattern is 18 db down from $\lambda/2$.)

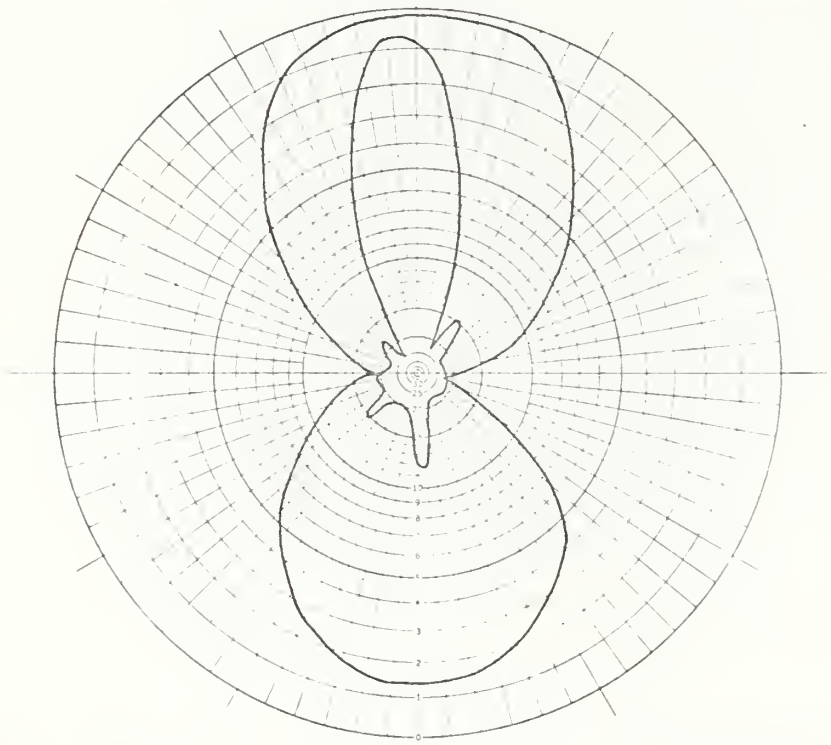

FIGURE 17. Radiation patterns of five gap antenna and resonant $\lambda/2$ dipole at 650 MHz. (TEM-line pattern is 7 db down from $\lambda/2$.)

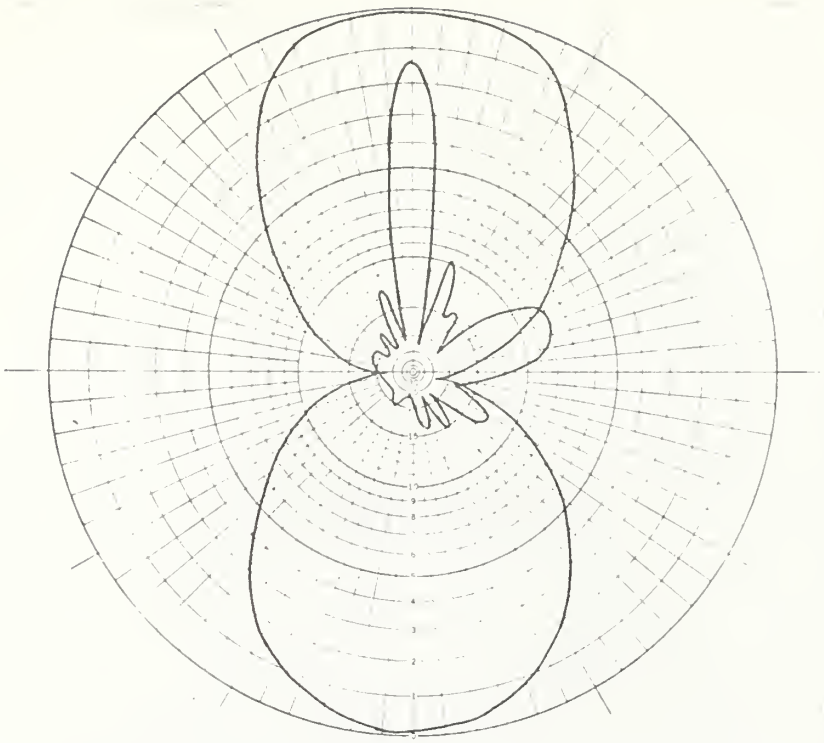

FIGURE 18. Radiation patterns of five gap antenna and resonant $\lambda/2$ dipole at 750 MHz

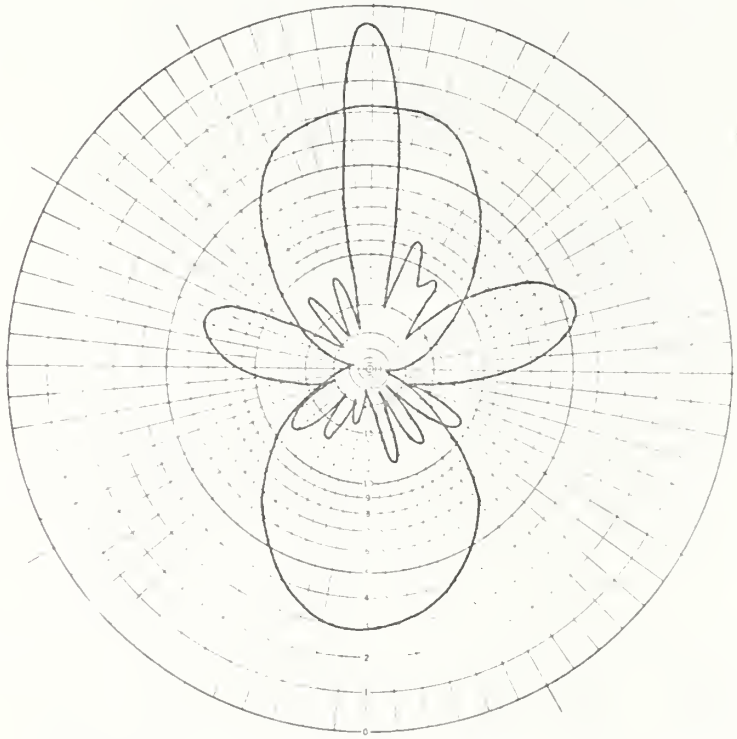

FIGURE 19. Radiation patterns of five gap antenna with double stub tuner in transmission line and resonant $\lambda/2$ dipole at 750 MHz

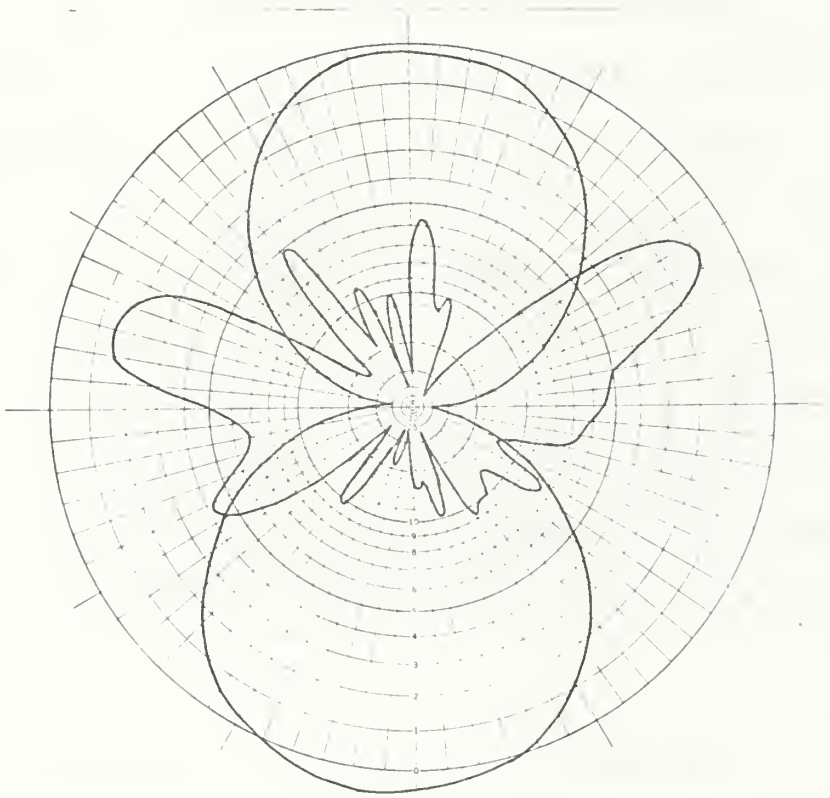

FIGURE 20. Radiation patterns of five gap antenna and resonant $\lambda/2$ dipole at 850 MHz. (TEM-line pattern is 17 db down from $\lambda/2$.)

IV. RESULTS

A. COMPARISON OF GAP REPRESENTATIONS

In Patak's study, the single gap parallel admittance characteristics were measured. In each case Patak's data indicated that the parallel gap conductance increased slightly with frequency which implies a decreasing shunt resistance. The data for the gap representation in this study indicates an increasing series resistance. Both the decreasing shunt resistance and the increasing series resistance characteristics indicate an increase in radiated power as frequency increases. This effect is shown in shown in Figure 13 as a gradual increase in radiated power as frequency increases. The results of this study confirm Patak's conclusions and further indicate that Copeland's half-loop hypothesis is not applicable for the single flush mounted gap.

B. ω-β DIAGRAM AND RADIATION CHARACTERISTICS

In using equation (13) to calculate the ω-β plot in Figure 11, one assumes an infinite number of periods or cells and that the radiation resistance is negligibly small. These assumptions greatly simplify the calculation without too much loss of information. The plot extends through the first (330-357 MHz) and the second (677-717 MHz) stopbands. The actual stopbands were somewhat broader due to the finite nature of the antenna and radiation resistance. The

actual stopband behavior may be observed from Figure 14 in terms of the large increase of reflected power in the stopband regions.

The frequency scanning characteristics may also be related to the ω-β diagram when used in conjunction with radiation patterns [14]. The objective in making radiation patterns for this study was to obtain gain information. The frequency scanning behavior was observed, however, to begin at 400 MHz in the endfire/backfire modes and progress to broadside in the 650-750 MHz range.

C. COMPARISON OF PATTERNS

Several radiation patterns of the five gap antenna were taken from 400 MHz to 850 MHz covering the first and second stopbands. The antenna was terminated with a variable short circuit in order to maximize the amount of radiation obtained. The most favorable pattern comparison was obtained at the design frequency, 750 MHz, with the addition of a double stub tuner in the transmission line from the antenna to the receiver. Patterns at other frequencies ranged from 5 db to 22 db below that of a resonant $\lambda/2$ dipole antenna. The highly attenuated patterns, with the exception of the pattern at the design frequency of 750 MHz, occurred at frequencies where the reflected power was either at a peak or very large. The periodic variations in the reflected power characteristic are possibly due to VSWR variations in the coaxial line and operation at frequencies where the reflected power is large should be avoided.

V. CONCLUSIONS AND RECOMMENDATIONS

It was found that the impedance characteristics of a single radiating gap may be found in a straightforward manner. The gap characteristics determined in this study indicate an increasing radiation resistance with frequency which support Patak's conclusions [9] and deny Copeland's small half-loop hypothesis for the single gap [1]. Current study of the radiation resistance of various size gaps has also shown that the radiation resistance increases with gap size as well as with frequency. Further study should be devoted to determining the gap size that optimizes the radiation resistance for a given frequency.

The ω-β diagram was useful in quickly predicting the operating characteristics of the five gap TEM-line antenna. It is recommended that radiation patterns be made with a five gap or similar TEM-line antenna terminated in its characteristic impedance to more closely correlate radiation angle with the ω-β diagram.

The pattern comparison measurement at the design frequency, 750 MHz, shows the five gap TEM-line antenna to be a low gain, highly directional antenna. Gains as high as 12.3 db above an isotropic antenna have been obtained with a flush mounted TEM-line antenna [3]. The patterns for the five gap TEM-line antenna at frequencies other than the design frequency were from 5 db to 22 db below the resonant

$\lambda/2$ dipole. These relatively low level patterns were probably due to impedance mismatch between the antenna and transmission line together with the small gap size (0.0625λ) which made the radiation resistance small. Also, the radiating gaps are inherently mismatched to the coaxial cable which causes standing waves to always be present on the antenna proper. Further study should be done with matching techniques as well as with various gap sizes to improve the gain of the antenna. Various arrays should also be studied to determine a range of radiation characteristics since the number of applications of such a versatile antenna is limited only by one's imagination.

LIST OF REFERENCES

1. Copeland, J. R., Analysis of the TEM-Line Antenna, PhD thesis, Ohio State University, 1969.

2. Electro Science Laboratory, Department of Electrical Engineering, Ohio State University, Technical Report 2147-2, Dual Beam Slotted TEM-Line Antennas, by T. E. Kilcoyne, 3 April 1967.

3. Electro Science Laboratory, Department of Electrical Engineering, Ohio State University, Technical Report 2341-1, The Slotted TEM-Line Antenna--A Low Profile, Beam Scanning, Traveling Wave Antenna, by T. E. Kilcoyne, 3 April 1967.

4. Electro Science Laboratory, Department of Electrical Engineering, Ohio State University, Technical Report 2147-4, Investigation of a Low Profile Flush Mounted Antenna, by personnel of the Electro Science Laboratory, 14 March 1967.

5. Electro Science Laboratory, Department of Electrical Engineering, Ohio State University, Technical Report 2341-2, Low Profile Antenna, by personnel of the Electro Science Laboratory, 23 May 1967.

6. Electro Science Laboratory, Department of Electrical Engineering, Ohio State University, Technical Report 2341-3, Interim Technical Report (Low Profile Antenna), by personnel of the Electro Science Laboratory, 11 December 1967.

7. Electro Science Laboratory, Department of Electrical Engineering, Ohio State University, Technical Report 2147-3, The Single Beam Slotted TEM-Line Antenna, by T. E. Kilcoyne, 10 March 1967.

8. Electro Science Laboratory, Department of Electrical Engineering, Ohio State University, Technical Report 2147-1, Introduction to the Slotted TEM-Line Antenna, by J. R. Copeland, 8 March 1967.

9. Patak, L. W., Admittance Characteristics of a Coaxial TEM-Line Antenna, MS thesis, United States Naval Postgraduate School, 1971.

10. Copeland, J. R., A Surface Mounted Slotted TEM-Line Antenna, paper presented at the 15th annual symposium on USAF Antenna Research and Development, Monticello, Illinois, October 1965.

11. Hewlett-Packard Company, Application Note 62, Time Domain Reflectometry, by members of the Hewlett-Packard Company staff, 1964.

12. Knorr, J. B., EE 3622 Notes, United States Naval Postgraduate School, Monterey, California, 1972.

13. R. F. Transmission Line Catalog and Handbook, Catalog Number TL-2, p. 33, Times Wire and Cable Company, 1970.

14. Oliner, A. A., Radiating Periodic Structures: Analysis in Terms of k vs ω Diagrams, short course presented at Polytechnic Institute of Brooklyn Graduate Center, Brooklyn, New York, 4 June 1963.

INITIAL DISTRIBUTION LIST

		No. Copies
1.	Defense Documentation Center Cameron Station Alexandria, Virginia 22314	2
2.	Library, Code 0212 Naval Postgraduate School Monterey, California 93940	2
3.	Asst. Professor R. W. Adler, Code 52Ab Department of Electrical Engineering Naval Postgraduate School Monterey, California 93940	2
4.	Asst. Professor J. B. Knorr, Code 52Ko Department of Electrical Engineering Naval Postgraduate School Monterey, California 93940	1
5.	LT Jerry Neal Layl, USN 1222 Spruance Road Monterey, California 93940	1
6.	CAPT Lowell W. Patak, USMC Rural Route 1 Stacy, Minnesota 55079	1
7.	LT Dale E. Schultz SMC 2833 Naval Postgraduate School Monterey, California 93940	1

DOCUMENT CONTROL DATA - R & D

(Security classification of title, body of abstract and indexing annotation must be entered when the overall report is classified)

1 ORIGINATING ACTIVITY (Corporate author)

Naval Postgraduate School
Monterey, California 93940

2a. REPORT SECURITY CLASSIFICATION
Unclassified

2b. GROUP

3 REPORT TITLE

The Impedance Characteristics of a Coaxial TEM-line Antenna

4 DESCRIPTIVE NOTES (Type of report and inclusive dates)
Master's Thesis; June 1972

5. AUTHOR(S) (First name, middle initial, last name)

Jerry Neal Layl

6 REPORT DATE
June 1972

7a. TOTAL NO. OF PAGES
41

7b. NO. OF REFS
14

8a. CONTRACT OR GRANT NO.

b. PROJECT NO

c.

d.

9a. ORIGINATOR'S REPORT NUMBER(S)

9b. OTHER REPORT NO(S) (Any other numbers that may be assigned this report)

10. DISTRIBUTION STATEMENT

Approved for public release; distribution unlimited.

11. SUPPLEMENTARY NOTES

12. SPONSORING MILITARY ACTIVITY
Naval Postgraduate School
Monterey, California 93940

13 ABSTRACT

The coaxial TEM-line antenna is a low-profile, lightweight, simply constructed antenna that can be easily mounted on a wide variety of conducting surfaces. It is a low to medium gain antenna element capable of operation in broadside or frequency scanning modes.

This paper presents a method of determining the impedance characteristics of a single flush mounted radiating gap.

Several radiation patterns are presented to illustrate beam shape and scanning. The Brillouin or ω-β diagram is used to relate the frequency scanning properties to periodic structure theory.

KEY WORDS	LINK A		LINK B		LINK C	
	ROLE	WT	ROLE	WT	ROLE	WT
TEM-line antenna						
Low profile antenna						
Traveling wave antenna						
Periodic structures						

Thesis
L339 Layl
c.1
135495
The impedance characteristics of a coaxial TEM-line antenna.